"Polar mutagenesis of bacterial transcriptional units using Cas12a"

Antoine Graffeuil[1], Bernt Eric Uhlin[1] and David A. Cisneros[1]*

[1]Department of Molecular Biology, Umeå University, Umeå, Sweden.

*Corresponding author david.cisneros@umu.se

Abstract

Bacterial genes are often organized in functionally related transcriptional units or operons. One such example is the *fimAICDFGH* operon, which codes for type I fimbriae in *Escherichia coli*. We tested the hypothesis that markerless polar mutations could be efficiently engineered using CRISPR/Cas12a in the *fim* operon. Cas12a-mediated engineering of a terminator sequence inside the *fimA* gene occurred with efficiencies between 10 and 30%, whilst other types of mutations, such as a 97 bp deletion, occurred with 100% efficiency. Our results showed that some of the obtained mutants, including one with a single base substitution at the *fim* locus, had decreased mRNA levels of *fimA*, suggesting that the regulation of the *fim* operon was disrupted. We corroborated the polar effect of these mutants by phenotypic assays and quantitative PCR, showing up to a 43 fold decrease in expression of genes downstream *fimA*. We believe this strategy could be useful in engineering the transcriptional shut-down of multiple genes in one single step. For bio-production in *E. coli*, this opens the possibility of inhibiting competing metabolic routes.

Short title: Polar mutagenesis with Cas12a

23 **Introduction**

24

25 The evolutionary success of operons has been attributed to their contribution to the organization of
26 metabolic pathways, which ultimately allowed organisms to become less dependent on exogenous
27 sources of organic compounds (1). Importantly this relationship was maintained during evolution
28 for many metabolic pathways and was probably enhanced by horizontal gene transfer (1). Genes
29 within operons are co-transcribed from a single promoter but it has been shown that the mRNA of
30 each open reading frame (ORF) has an independent folding from their neighbouring genes and this
31 feature directly influences its translation efficiency (2). Other features regulating operon expression
32 and function in *cis* include attenuators, terminators and processive aniterminators (reviewed in
33 (3,4)). All these elements of regulation depend on the formation of secondary RNA structures.

34 We asked ourselves if sequences with such a tendency to generate secondary structures could be
35 easily engineered in the *E. coli* chromosome using CRISPR/Cas technologies. CRISPR/Cas
36 genome editing in *E. coli* (5), opened the possibility of marker-less genetic engineering with single
37 base resolution. Therefore, it is possible to now generate multi-scale libraries of mutants in a few
38 days (6). The objective of the following study was to design a strategy to shut-down the
39 transcription of entire operons using a synthetic terminator sequence (7) in *E. coli*.

40

41 The possibility of easily controlling entire transcriptional units would serve multiple purposes for the
42 bio-production of compounds using synthetic metabolic routes. For example one aspect poorly
43 appreciated in synthetic biology is metabolic burden (8). Protein synthesis has been calculated to
44 be the most expensive step (ATP-wise) involved in cell growth, compared to the biosynthesis of its
45 building blocks (amino acids) which uses only a small fraction of ATP (9). Therefore shutting down
46 the synthesis of unnecessary operons during specific growth conditions could contribute
47 significantly to balance the burden while expressing heterologous operons. Another example is

48 shutting down or the re-direction of competing metabolic routes (10) during bio-production from
49 heterologous operons. To that effect, the bioinformatic analysis of competing or converging
50 metabolic routes will be essential (11). Another interesting application would be the removal of
51 virulence factors and antibiotic resistance genes as a potential antimicrobial strategy (14). These
52 type of genes also tend to cluster together in so called pathogenicity islands. Therefore, the
53 strategy presented in the following study opens another possibility to investigate, with one step, the
54 effect of competing transcriptional units arranged in operons on metabolic burden and compound
55 biosynthesis.
56

57 Type one fimbriae are adhesive surface appendages present mainly in *Enterobacteriaceae* that
58 were first shown to agglutinate red-blood cells (15). They are composed of a main pilin subunit
59 repeated in the order of hundreds to thousands and are assembled at the surface by an outer
60 membrane usher. At the tip of the filament the so called minor pilins are assembled in a specific
61 order. The most distal pilin to the cell (FimH) functions as an adhesin (16,17). In the case of *E. coli*
62 type I fimbriae the FimH adhesin is inhibited by D-mannose residues and α-methyl-mannoside and
63 they recognize mannosylated receptors (16–18). Its role in virulence in uropathogenic strains of *E.*
64 *coli* has been established for a long time (19,20). However, its role in mammalian persistent
65 intestinal colonization has only been recently shown to be essential for the case of uropathogenic
66 *E. coli* (21). It has not yet been studied, how each of the several fimbrial systems present in
67 symbiotic *E. coli* strains (22) contributes to intestinal colonization *in vivo*.
68

69 The *fim* operon is a good system to test an engineered polar effect, for several reasons: Firstly, the
70 architecture of the *fim* operon is such that the gene coding for the major and most abundant
71 component of the pilus is the first to be transcribed, followed by the assembly machinery. This
72 gives the advantage that disruption of the first gene inactivates functionality of the fimbriae
73 complex and any polar effect would disrupt the function of the subunits important for fimbriae

74 assembly. Secondly, the levels of *fim* transcription are chiefly determined by an invertible element
75 upstream of the promoter (*fimAp*), which acts as an ON/OFF switch. The regulation of the
76 mannose-dependent adhesion of type I fimbriae is complex, and has been studied *in vitro* for
77 decades. It has been shown to be regulated by various genes including NanR and NagC (trough
78 sialic acid and GlcNAc) (23), Lrp, (24,25), H-NS (26) and IHF (27). All these elements mainly
79 regulate the frequency of inversion of the invertible switch. The molecule (p)ppGpp also regulates
80 the *fim* switch (28). Therefore, it should be possible to quantify a polar effect in the *fim* operon by
81 measuring the transcription of genes downstream of *fimA*.
82

83 In this study we introduce a terminator sequence with a strong secondary structure within the *fim*
84 operon to disrupt its transcription. We showed that this sequence is easy to introduce by
85 CRISPR/Cas12a engineering and that the assembly machinery of *E. coli's* type I fimbriae can be
86 turned off using this polar mutagenesis strategy.
87

88

89 **Results**

90 **Design of *fimA-targeting* crRNA and donor oligos**

91

92 We set out to disrupt the *fim* operon using Cas12a to introduce a range of different markerless
93 mutations in the *fimA* gene, including the insertion of a terminator sequence (Fig. 1). We designed
94 a CRISPR RNA (crRNA) targeting the *E. coli fimA* gene. To introduce polar and nonpolar
95 mutations in the *fim* operon we designed two complementary oligos for each mutation to form
96 dsDNA donor molecules for homologous recombination. The recombination of these oligos
97 disrupts the binding site of the Cas12a-crRNA complex and permits the positive selection of mutant
98 cells (29).

99

100 To introduce a premature stop codon in the *fimA* gene, we designed dsDNA donor oligos in which
101 a single bp change disrupted the PAM sequence adjacent to the target of the designed *fimA* crRNA
102 (crRNA1) and introduced a stop codon (TAA) after 106 bp of the start codon ($fimA_{A106T}$). To
103 introduce a deletion in the *fimA (ΔfimA)* gene, we designed dsDNA donor oligos containing
104 homology recombination sequences upstream and downstream of the crRNA recognition site to
105 delete 97 bp introducing a stop codon after 75 bp after the start codon (Fig. 1).

106

107 To engineer a polar mutagenesis strategy, we designed two different donor oligos introducing a
108 terminator sequence in the *fimA* gene. The first pair of oligos contained the exact same sequences
109 for homologous recombination as the deletion donor oligos but including the L3S2P56 terminator at
110 nucleotide position 75 after the start codon ($fimA_{75}$*::L3S2P56*, called here Term1). The second
111 donor oligos were similar but the upstream homologous region corresponded to the leader of the
112 *fimA* gene. Therefore, these oligos introduce a terminator sequence at the start codon
113 ($fimA_{1}$*::L3S2P56*, called here Term2).

114

115 **Mutagenesis of the *fimA gene***

116

117 Terminator sequences have a strong tendency to form secondary structures and therefore we
118 asked ourselves if such sequences could serve as DNA donors for CRISPR/Cas12a mutagenesis.
119 To test this we simply electroporated *E. coli* cells carrying the plasmid pKD46-Cas12a (29) with the
120 annealed dsDNA donor oligos and a plasmid encoding crRNA1. We analysed transformants by
121 colony PCR using oligos that amplify a segment of the *fimA* gene surrounding the site of crRNA
122 targeting. For the stop codon mutant ($fimA_{A106T}$) obtained with crRNA1, we analysed five colonies.
123 The size of the PCR fragment did not appear to change as compared to wild type (WT) *E. coli* (Fig
124 2). We purified these PCR products and submitted them for Sanger sequencing. Four of the
125 products showed the specific T->A substitution that introduces a premature stop codon. For the
126 *ΔfimA* mutant, the PCR fragment showed a noticeable change in migration pattern compared to
127 WT (Fig 2). Ten out of ten colonies picked showed the deletion (S1 Fig.). For mutants with the
128 insertion of a terminator sequence only three out of ten and one out of ten colony PCRs showed a
129 change in migration pattern for the Term1 and Term2 mutations, respectively (Fig. 1 and S1 Fig).
130 Altogether these results indicate that the engineering of terminator sequences is possible but with
131 lower success rates compared to the highly efficient engineering of a single base substitution and a
132 deletion.

133

134 **Phenotypic analysis of *fimA* mutants**

135

136 To characterise the effect of the different mutations, we verified the functionality of the *fim* operon
137 gene products by a phenotypic assay. We performed agglutination assays of *Saccharomyces*
138 *cerevisiae* cells (Fig 3A-C). Overnight cultures of WT and *fimA* mutants *E. coli* strains were mixed

139 with a drop of a yeast suspension over a glass plate. With WT *E. coli* this led to agglutination of the
140 yeast cells, which appeared as white, macroscopically visible aggregates (Fig 3D). Contrastingly,
141 mixing *Shigella flexneri* M90T, which is known not to produce fimbrial genes when grown in tryptic
142 soy agar (30), presented no yeast aggregates (Fig 3E). Mixing each of our *fimA* mutants with the
143 yeast suspension produced no agglutination (Fig 3F-I). There was no difference between the stop
144 codon mutant ($fimA_{A106T}$), deletion and terminator mutants (Ter1 and Ter2), which suggests that
145 the disruption of even one base introducing a stop codon was enough to alter the expression of the
146 *fim* operon.
147

148 **Plasmid trans-complementation of the *fimA* mutants**

149

150 To verify the efficiency of the different mutations in exerting a polar effect, we verified the
151 functionality of the *fim* operon by a phenotypic assay in WT and mutant strains carrying a plasmid
152 expressing *fimA* (Fig. 4). Each strain was transformed by the trans-complementing plasmid and an
153 empty vector as negative control. WT *E. coli* carrying the empty vector agglutinated *S. cerevisiae*
154 as expected. Similarly, the expression of plasmid encoded *fimA* had no effect on the agglutination
155 reaction (Fig 4A-B), suggesting that neither of the plasmids had an impact on agglutination. Trans-
156 complementation of both the stop codon (*fimAA106T*) and deletion *fimA* mutants resulted in yeast
157 agglutination (Fig 4C-D and Fig 4E-F), suggesting that the mutations did not introduce any effect
158 on genes downstream of *fimA*, which code for the assembly machinery, and that expression of a
159 functional copy of this gene rendered these strains agglutination-positive. In contrast, the strains
160 carrying the empty vector were agglutination-negative. Trans-complementation of both Term1 and
161 Term2 mutants with the empty vector or the plasmid expressing *fimA,* resulted in no yeast
162 agglutination (Fig 4G-H and Fig 4I-J). This suggests that the functionality of the *fim* operon was
163 completely disrupted downstream of *fimA* in these two mutants and suggested that the introduction
164 of the L3S2P56 terminator functionally disrupted the transcription of the entire *fim* operon.

165

166 **Measurement of mRNA levels of *fimA* and *fimI***

167

168 We wanted to quantify the extent of a polar effect in all the mutants obtained. We used qPCR to
169 measure the levels of *fimA* and *fimI* mRNA. We designed two sets of primers that allowed for the
170 estimation of the levels of these two genes (Fig 1B). We performed qPCR using as template cDNA
171 derived from mRNA obtained from *E. coli* cultures grown in the same conditions as those used for
172 the phenotypic assays. First, we estimated the amount of the *fimI* mRNA relative to *fimA.* This
173 represents an unbiased measurement that does not depend on the ON/OFF state of the *fimAp*.
174 Relative expression of *fimI* in WT *E. coli* was ~2.5 times lower to *fimA* (Table 1). The median
175 relative expression of *fimI* in the stop and deletion mutants was lower but in the same order of
176 magnitude (Fig 5A). The median relative expression of *fimI* in the Term1 and Term2 mutants was
177 considerably lower (Fig 5A). The relative expression fold change for the Term1 and Term2 mutants
178 was 9 and 43 fold, respectively (Table 1). These results suggest that at least an estimated 9 fold
179 change in expression is sufficient to disrupt the functionality of the *fim* operon downstream of *fimA*.

180 We wanted to measure the levels of *fimI* and *fimA* mRNA levels with respect to housekeeping
181 genes. We designed sets of primers for the housekeeping genes *hcaT* and *cysG*, which have been
182 shown to have stable expression (31). We obtained the average ΔCt with respect to these two
183 genes and normalized it to the WT control performed the day of the experiment. The levels of *fimA*
184 varied in all the mutants as well as the levels of *fimI*. For the stop codon mutant, the deletion
185 mutant and the Ter1 mutant the levels of *fimA* mRNA were lower than the WT (Fig 5B). The levels
186 of *fimI* were lower for all the mutants, with the Ter1 and Ter2 mutants having the most severe
187 defects compared to WT(Fig 5B).

188

189 We were puzzled by the small but measurable changes of mRNA levels in the stop and deletion

190 mutants in *fimA* mRNA(Fig. 5B). To further investigate this phenomenon, we decided to create two
191 different stop codon mutants. We co-introduced in *E. coli* plasmids encoding crRNA2 and crRNA3
192 (Fig 1) with donor template oligos introducing a stop codon instead of the PAM sequence into *E.*
193 *coli* carrying the plasmid pKD46-Cas12a. For crRNA2 the donor oligos introduced the mutations
194 T103A, T104A ($fimA_{T103A,T104A}$) to disrupt the PAM sequence. For crRNA3 the donor oligo introduced
195 the mutations A158T,A159T, A160T,C161A, C162A ($fimA_{A158T,A159T,A160T,C161A,C162A}$). Two clones of
196 each of these mutants were selected and analysed by qPCR measurements of *fimI* and *fimA.* The
197 median relative expression of *fimI* to *fimA in* these two new mutants was also lower but in the same
198 order of magnitude of mutants carrying the allele $fimA_{A106T}$ (Fig 5A, orange and yellow circles). This
199 result suggests that the reduced levels of *fimA* expression are consistent in all three stop codon
200 mutants. Moreover, these results indicate that the lower *fimA* mRNA levels are not caused by an
201 off-target effect of crRNA1.
202

203 **Observation of a *fimA* terminator mutant by AFM**

204

205 We wanted to observe the formation of fimbriae by Atomic Force Microscopy (AFM) and
206 agglutination in previously described favourable conditions. Fluorescence microscopy
207 measurements have shown an increase of fimbriae in static cultures of *E. coli* strain MG1655 (32).
208 We grew WT *E. coli* and the Ter2 mutant expressing *fimA* from a plasmid on static cultures to
209 observe if there was any formation of fimbriae. To prepare the AFM samples in a way that it
210 introduced the least amount of manipulations, we diluted the static culture in deionized water to an
211 OD600 of 0.05 and we immobilized a drop of this suspension on freshly cleaved mica for 20
212 minutes. After the incubation period the mica was gently washed with more deionized water. In the
213 wild type strain expressing plasmid-encoded *fimA*, we observed bacteria showing the classical type
214 I fimbriae (Fig. 6A and 6A inset). However in the Ter2 mutant expressing plasmid-encoded *fimA* we
215 did not observe any formation of fimbriae (Fig. 6A). In some cells, only the formation of flagella

216 could be observed (Fig.6A inset). To confirm the absence of functional fimbriae in this mutant, we
217 repeated the yeast agglutination assay after static growth conditions (Fig. 6B). As a negative
218 control we incubated this time the wild type strain with α-methyl-mannoside. The wild type strain
219 expressing plasmid-encoded *fimA* was agglutination-positive as shown in Fig. 4. However using
220 the same strain pre-incubated with α-methyl-mannoside completely abolished agglutination. This
221 confirms that agglutination is mediated by the mannose-dependent type I fimbriae encoded in the
222 *fim* operon. Agglutination by the Ter2 mutant expressing plasmid-encoded *fimA* did not
223 complement agglutination after having grown in static conditions and the agglutination reaction
224 appeared as the α-methyl-mannoside negative control. All these results confirm that the Ter2
225 mutant has a *fim* negative phenotype even when *fimA* is expressed in *trans*.
226

227 **Table 1. Relative levels of *fimI* to *fimA* mRNA.**

Strain	Median Δct (*fimI* - *fimA*)*	Median Δct (*fimA* - *fimI*)	~Fold change inhibition
WT	0.39	2.6	1
Stop codon	0.10	9.8	4
ΔfimA	0.17	5.8	2
Term1	0.04	23.3	9
Term2	0.009	111.4	43

228 **Table1. Relative levels of *fimI* transcript with respect to *fimA*.** The median ΔCt values are
229 shown as in **Fig 5A**. The fold change was calculated by dividing the median ΔCt (*fimI* – *fimA*) of
230 each mutant by the median value in the wild type.

231

232 **Discussion**

233

234 CRISPR/Cas technologies have become part of routine work in many laboratories. For the
235 synthetic biology field these techniques opened the possibility of quickly engineer chromosomal
236 loci. For biotechnological purposes, it also opens the possibility to decrease the use of plasmids to
237 produce heterologous enzymes. Plasmids can be lost and impose extra metabolic burdens and
238 regulatory burdens that have to be taken into account when fine-tuning bio-production (reviewed in
239 (8)). One proposed approach is to iteratively test the effect of engineered mutations in strains to
240 optimize this process (33). However the effect of a mutation in a system often carries unpredictable
241 or poorly controlled consequences. In *E. coli*, 63% of its genes are organized in operons (34) and
242 40% are organised in uber operons (35). In both of these organisation levels, genes tend to be
243 related by functional conservation across bacterial genomes (35). The possibility to
244 transcriptionally shut-down with one step a whole operon could contribute to the quick design and
245 testing of strains with more predictable outcomes if regulons and uber operons were taken into
246 account.

247

248 In this study we used an artificial terminator sequence to shut down the transcription of the *fim*
249 operon. This designed artificial sequence has an extended secondary structure that has been
250 shown to improve transcriptional termination (7). We did not know whether such secondary
251 structures could impede the recombination process in the context of the donor homology
252 recombination oligonucleotides used for CRISPR/Cas genome engineering. The predictable
253 outcome from inserting this sequence in the *fim* operon is the premature transcriptional termination
254 of the genes coding for the type I fimbriae assembly machinery. Our results indeed showed a
255 reduction of up to 43 fold in the expression of the *fim* machinery as measured by the expression of
256 *fimI.*

257

258 The efficiency of genome engineering strains has been shown to depend on the efficiencies of
259 gRNAs to direct Cas9 DNA cleavage and donor oligos (6). Using the same crRNA (crRNA1) to
260 generate several mutations at the same target sequence we saw that each mutation was produced
261 with efficiencies ranging from 10% to 100%. However the donor oligonucleotides varied in
262 homology arms and secondary structure. Therefore our results suggest that, as suspected, these
263 two parameters are important for bacterial genome engineering. Despite these differences we
264 could readily find mutants with inserted terminator sequences. Among the 582 terminator
265 sequences characterised by Chen *et al.*, we decided to use an artificial terminator sequence
266 (L3S2P56) that showed to have low recombination rates (7), which would ensure more stability
267 within the *E. coli* chromosome. However we did not know whether this would decrease the
268 recombination mediated by homology arms upstream and downstream of the terminator sequence.
269 Our results show that this sequence was easily engineered using the Cas12a-encoding plasmids
270 designed by Yan *et al.* (29). These plasmids are easy to use and allow multiple rounds of
271 mutagenesis similar to previously reported Cas9 approaches (6). Cas12a also brings the
272 advantage that it processes its own crRNAs, which we think will allow certain flexibility in the future
273 when dealing with organisms with poorly characterised promoter sequences. All together this study
274 shows that it is possible to shut down the expression of a whole operon using an artificial
275 terminator. This approach could be complementary to other approaches that allow the
276 transcriptional repression of multiple genes such as the use of multiple gRNAs for transcriptional
277 repression (12) or the deletion of large genomic stretches (13). The use of Cas12a also facilitated
278 genome engineering, because its PAM sequence NTTT (AAAN in the bottom strand) can be easily
279 mutated to introduce a stop codon. Indeed here we showed that a single base substitution
280 ($fimA_{A106T}$) disrupted PAM recognition and allowed the selection of *fimA* mutant strains.
281

282 The *fim* operon was an ideal study case because the phenotype is macroscopically observable and
283 the characterisation of the *fimA* mutants by yeast agglutination produced easy to interpret results.
284 Moreover, the extent of fimbriation is directly correlated to the state of the switch inside *fimAp* (32),

285 therefore for every *fimA* transcript observed the presence of a *fimI* transcript reflects the polarity of
286 the mutants generated here. Indeed, insertion of a terminator sequence abolished the trans-
287 complementation by a plasmid-encoded *fimA* gene. Less predictable phenotypes were obtained by
288 measuring the relative expression of *fimI* to *fimA* in typical laboratory conditions. Three out the four
289 mutants that were generated in this study, both polar and nonpolar, had reduced median levels of
290 *fimA transcript* and of the ratio *fimI/fimA* transcripts. This includes a single base substitution that
291 introduces a stop codon *(fimA$_{A106T}$).* Several possible explanations exist to accommodate this fact.
292 For example, it is known that ribosome binding protects mRNAs from RNase E degradation (36).
293 Therefore, one possible explanation would be that the premature stop codon introduced in
294 *fimA$_{A106T}$* and in the deletion mutant induces the premature release of ribosome (37,38) and at the
295 same time exposes the *fimA* transcript to degradation. Another more complicated involves the
296 stalling of ribosomes during translation, which may induce mRNA cleavage next to or at a stop
297 codon (39). An initial cleavage event could lead to further degradation by classical mRNA decay
298 pathways. However this could only make sense if the folding of the *fimA* mRNA would be
299 compromised and stalling would be induced by the mutations designed here. This can also be put
300 in the context of the recent discovery that the mRNA of individual genes within operons have a
301 unique secondary structure (2). Deletions smaller than a whole gene could affect the folding of an
302 individual genes' mRNA within an operon. Another possibility would be that there would be some
303 kind of positive feedback on type I fimbriae expression or functionality. On the conditions that we
304 assayed *fimA* expression, that is rich medium at 37 C, switching off dominates on *fimAp* (40).
305 Therefore, any kind of feedback would quickly result in *fimA* expression inhibition. Another
306 possibility would be that the mutation introduced in this study interferes with a differential stability
307 within *fim* genes' transcripts, which is an important element for other fimbrial systems (e.g, the *pap*
308 fimbrial operon from uropathogenic *E. coli*) (41). One final possibility is that expression of a
309 functional type I fimbriae system confers a growth advantage (32,42), although this has only been
310 proposed for static cultures. Alternatively, the peptide products of the stop codon mutants (~35
311 amino acids long and hydrophobic) could also be partially toxic and induce the selection of cells
312 with the *fim* switch in the off state. Although this would not apply to the terminator insertion at

313 position 1 (Ter2) mutant, for which there should not be any partial *fimA* peptide product. Further
314 studies will be needed to clarify the role of the three stop codon mutants and deletion on the
315 expression of *fimA.* However, our results show that even a single nucleotide substitution can have
316 subtle but measurable changes at the transcriptional level within an operon when measured in
317 typical laboratory conditions.

318 The chromosome of *E. coli* encodes multiple fimbrial systems. However, in the conditions used in
319 this study, only the *fim* type I fimbriae are functional (22). The results shown in this study open the
320 possibility of quickly generating *E. coli* strains in which each fimbrial operon is inactivated. This
321 could be useful to see if any of these systems is essential under a particular growth condition.
322 Another future direction of interest is to characterise the effect of other *fimA* stop codon mutants on
323 the stability of its transcript. It would be crucial to determine if the effects observed here are gene
324 specific or can occur in many other premature stop codon mutants. This is important in the light
325 that introducing a premature stop codon is the easiest form to disrupt a gene using markerless
326 techniques such as Cas9- or Cas12a-mediated mutagenesis.
327

328 In summary, in this study we show that Cas12a can be used to introduce markerless insertions in
329 *E. coli* in one step and that this insertion can have strong secondary structures such as terminator
330 sequences without excessively compromising the efficiency of the process. This approach allows
331 the transcriptional shut-down of whole operons as demonstrated for the case of the *fim* type I
332 fimbriae system. More importantly, this strategy can be used to easily test the importance of entire
333 operons for the physiology of *E. coli* or its effect in the design of novel or artificial biosynthetic
334 pathways.

335 **Materials and Methods**

336

337 **Cas12a Mutagenesis.** To design Cas12a crRNA targeting *fimA* with no off-targets in *E. coli*

338 MG1655 (43), we used the webtool Chop-Chop (44) and crRNAs ranking 1, 2 and 4 were selected
339 due to its closeness to the start codon. To introduce all the mutations designed in this study we
340 used the plasmids designed by Yan *et al.* (29) and followed their protocol with some modifications.
341 Cloning of crRNAs was done by annealing forward and reverse oligos at 95 °C and ramping the
342 temperature down at 2.55°C/min. The oligos were then phosphorylated using polynucleotide
343 kinase (ThermoFisher). The plasmid pAC-crRNAred (29) was digested with BsaI-HF (New England
344 Biolabs), dephosphorylated with FastAP (ThermoFisher) and ligated to the annealed oligos. Donor
345 oligos were treated in the same way as crRNA oligos and their annealing was verified as
346 suggested by König *et al.* (45). The night before the experiment we grew *E. coli* MG1655 carrying
347 plasmid pKD46-Cas12a at 30 °C starting from a glycerol stock. The day of the experiment, 100 µl
348 of overnight culture were transferred to a new agar plate with 0.2% arabinose and 4 h later
349 electrocompetent cells were prepared using the "rapid" protocol (46). These cells were co-
350 transformed by plasmids carrying one crRNA and an annealed pair of donor oligos. As a control
351 transformation we used a crRNA targeting the gene coding for GFP. Colony PCR was then
352 performed on transformants for genotyping. Each colony was resuspended in 20 µl water and
353 boiled for 5 min. One µl of this sample was used as template for PCR. Agarose gel electrophoresis
354 or Sanger sequencing was followed to determine the number of mutants. At least two independent
355 colonies of each mutant were selected for further analysis. After mutagenesis was confirmed by
356 sequencing, the strains were cured from the plasmids following the recommendations of Yan *et al.*
357 (29). We observed that this process had a 100% efficiency by growing the cells at 37 °C in 5%
358 sucrose in very rich medium such as YT2X. Glycerol stocks were then prepared for each clone.
359 The structure of the L3S2P56 terminator was calculated with the Vienna websuite (47) and
360 visualised with Forna (48).
361

362 **Agglutination assay.** To observe yeast agglutination, wild type or mutant MG1655 was grown
363 overnight for 16 h on Luria agar plates as described before (49). A 1 ul plastic loop was used to
364 take a colony from the plate and mixed with 200 µl of a *Saccharomyces cerevisiae* suspension at

365 OD_{600} 5 prepared from refrigerated baker's yeast (Lidl Sverige). The loop was used to gently mix
366 the two cell populations and the appearance of white flocculated aggregates could be observed for
367 the wild type strain in less than 30 seconds. *Shigella flexneri* 5A M90T *was* used as a negative
368 control (50). To perform this assay from static cultures, 10 µl from strains grown overnight in static
369 broth (20 ml tryptic soy broth) were mixed with 200 µl of a *Saccharomyces cerevisiae* suspension
370 at OD_{600} 5. In the case of the wild type strain expressing plasmid-encoded *fimA*, the agglutination
371 took approximately 2-5 min under this conditions.. As a negative control, 10 µl of a 3% (w/v)
372 solution of α-methyl-mannoside was added to a 10 µl suspension of wild type *E. coli* and pre
373 incubated for 1 minute before agglutination.
374

375 **RNA isolation.** To isolate RNA we used the modified method described by Blomberg *et al.* (51)
376 with one further modification. Namely, we grew cells in the same conditions as for agglutination
377 assays (overnight on Luria agar plates) on a lawn. The equivalent to half a plate was scraped and
378 dissolved immediately in DEPC treated water with 10% SDS, 20 mM sodium acetate pH 4.8 and
379 10 mM EDTA and flash frozen in liquid nitrogen. Frozen cells were thawed and lysed by incubating
380 the samples for 5 min at 65 ºC. Total RNA was extracted by the hot-phenol method (51). Residual
381 DNA was digested by DNase I (ThermoFisher; 1 U/µg RNA, 60 min, 37 ºC) in the presence of
382 RNase inhibitor (Ribolock, ThermoFisher Scientific; 0.1 U/µl) followed by a cleaning step using
383 phenol/chloroform/isoamyl alcohol (25:24:1) and precipitation with ethanol, 0.1 M sodium acetate
384 pH 5.5 and 20 µg of glycogen (ThermoFisher). Removal of residual DNA was verified by PCR
385 using *fimA* oligos. Complementary DNAs (cDNAs) were prepared from each RNA sample using the
386 RevertAid kit (ThermoFisher) according to the manufacturer instructions. As a control of DNA
387 contamination we prepare for each sample a sample without reverse transcriptase (-RT sample).
388

389 **qPCR analysis.** To perform qPCR we used SYBR Green master mix (ThermoFisher) according to
390 the manufacturer instructions. To analyse the expression of *fimA*, *fimI*, *hcaT* and *cysG*, we

391 designed specific oligos using primer BLAST (Table 2). We used an iCycler iQ5 (Bio-Rad) and for
392 each gene cDNAs generated from bacteria grown on plates and as a control we produced a
393 sample without reverse transcriptase (-RT) using the exact same RNA. We verified that for each
394 qPCR experiment we did not find any detectable signal in the -RT sample. Denaturation curves
395 were also acquired to verify the presence of a single product. We performed these controls for
396 every single biological replicate. To verify the linearity of each primer we diluted the cDNA obtained
397 from wild type *E. coli*, which always contained the highest amounts of *fimA and fimI* and verified
398 that 10 times dilutions steps had a slope close to -3.3. To analyse qPCR data we used the iQ5
399 optical system software (Bio-Rad) obtained the ΔCt from the suggested values of the software. We
400 verified in any case manually that changes in the threshold did not affect or bias the results. Each
401 measurement was quantified using the following formula: Δct=2^(ct1-ct2), where ct is the threshold
402 crossing value at which the SYBR green fluorescent signal appears. In the case of the *fimI* to *fimA*
403 ratio reported in Fig. 5A we simply report the ΔCt without any transformation. Although Ct values
404 varied across experiments, the *fimI* to *fimA* ΔCt was, in our hands, consistent across experiments
405 within one order of magnitude. To normalize the data of *fimA* and *fimI* against housekeeping genes
406 we obtained the ΔCt of each sample against the ct value of *cysG* and *hcaT* and the average of the
407 two values was obtained. The average ΔCt values of each sample was normalized against the ΔCt
408 of the wild type strain as a percentage. The ratio of the *fimI* to *fimA* expression was obtained by
409 dividing their normalized ΔCt values and expressed as a percentage.
410

411 **AFM.** To prepare AFM samples, punch-holed 1 cm pieces of muscovite mica were immobilized on
412 metal supports using double sided tape. The static cultures were diluted ten times in ultrapure
413 milliQ water. A drop of 100 µl from the diluted bacterial suspension was afterwards placed on the
414 mica right after cleaving it with laboratory tape. The suspension was incubated for 20 minutes to
415 allow adhesion of bacteria and the liquid was exchanged three times with ultrapure milli Q water.
416 The samples were placed in the chemical hood and left to dry for a minimum of 5 min. The
417 presence of bacteria on the mica was verified using an optical system mounted on the AFM

418 (Bruker) and a random area was selected for imaging. The AFM imaging was performed in a
419 MultiMode8 instrument (Bruker) in force tapping mode using the ScanAsyst software at a rate of 1
420 Hz and using ScanAsyst tips with a nominal spring constant of 0.4 N/m. Images shown in Fig. 6
421 depict the error signal generated by the piezo (J scanner).

422 **Acknowledgements**

423

424 We thank the support of the Carl Tryggers Stiftelse för Vetenskaplig Forskning (projects CTS 15-96
425 and CTS18-65 awarded to David A. Cisneros), the Kempestiftelserna (projects JCK-1724 awarded
426 to Bernt Eric Uhlin and SMK 1860 awarded to David A. Cisneros). We also want to thank Ramon
427 Cervantes Rivera for helping with RNA purifications. We also thank Aster Assefa for her technical
428 assistance in qPCR and the creation of deletion mutants and Andrea Puhar for critical reading.

429

430

431 **References**

432 1. Fondi M, Emiliani G, Fani R. Origin and evolution of operons and metabolic pathways.
433 Research in Microbiology. 2009 Sep 1;160(7):502–12.
434 2. Burkhardt DH, Rouskin S, Zhang Y, Li G-W, Weissman JS, Gross CA. Operon mRNAs are
435 organized into ORF-centric structures that predict translation efficiency. Elife.
436 2017;6:e22037.
437 3. Merino E, Yanofsky C. Transcription attenuation: a highly conserved regulatory strategy
438 used by bacteria. Trends in Genetics. 2005 May 1;21(5):260–4.
439 4. Goodson JR, Winkler WC. Processive Antitermination. Microbiology Spectrum. 2018 Oct
440 5;6(5):RWR-0031-2018.
441 5. Jiang W, Bikard D, Cox D, Zhang F, Marraffini LA. RNA-guided editing of bacterial
442 genomes using CRISPR-Cas systems. Nature biotechnology. 2013 Mar;31(3):233–239.
443 6. Zerbini F, Zanella I, Fraccascia D, König E, Irene C, Frattini LF, et al. Large scale validation
444 of an efficient CRISPR/Cas-based multi gene editing protocol in *Escherichia coli*. Microbial
445 cell factories. 2017;16(1):68.
446 7. Chen Y-J, Liu P, Nielsen AAK, Brophy JAN, Clancy K, Peterson T, et al. Characterization of
447 582 natural and synthetic terminators and quantification of their design constraints. Nature
448 Methods. 2013 Jun;10(7):659–664.
449 8. Wu G, Yan Q, Jones JA, Tang YJ, Fong SS, Koffas MAG. Metabolic Burden: Cornerstones
450 in Synthetic Biology and Metabolic Engineering Applications. Trends in Biotechnology.
451 2016 Aug 1;34(8):652–64.
452 9. Russell JB, Cook GM. Energetics of bacterial growth: balance of anabolic and catabolic
453 reactions. Microbiol Mol Biol Rev. 1995 Mar 1;59(1):48–62.
454 10. Solomon KV, Moon TS, Ma B, Sanders TM, Prather KLJ. Tuning Primary Metabolism for
455 Heterologous Pathway Productivity. ACS Synth Biol. 2013 Mar 15;2(3):126–35.
456 11. Kuwahara H, Alazmi M, Cui X, Gao X. MRE: a web tool to suggest foreign enzymes for the
457 biosynthesis pathway design with competing endogenous reactions in mind. Nucleic Acids

458 Res. 2016 Jul 8;44(W1):W217–25.
459 12. Cress BF, Toparlak ÖD, Guleria S, Lebovich M, Stieglitz JT, Englaender JA, et al.
460 CRISPathBrick: modular combinatorial assembly of type II-A CRISPR arrays for dCas9-
461 mediated multiplex transcriptional repression in *E. coli*. ACS synthetic biology.
462 2015;4(9):987–1000.
463 13. Su T, Liu F, Gu P, Jin H, Chang Y, Wang Q, et al. A CRISPR-Cas9 Assisted Non-
464 Homologous End-Joining Strategy for One-step Engineering of Bacterial Genome.
465 Scientific Reports. 2016 Nov 24;6(1):1–11.
466 14. Bikard D, Euler CW, Jiang W, Nussenzweig PM, Goldberg GW, Duportet X, et al. Exploiting
467 CRISPR-Cas nucleases to produce sequence-specific antimicrobials. Nat Biotechnol. 2014
468 Nov;32(11):1146–50.
469 15. Duguid JP, Smith IW, Dempster G, Edmunds PN. Non-flagellar filamentous appendages
470 ("fimbriae") and haemagglutinating activity in *Bacterium coli*. The Journal of pathology and
471 bacteriology. 1955;70(2):335–348.
472 16. Jones CH, Pinkner JS, Roth R, Heuser J, Nicholes AV, Abraham SN, et al. FimH adhesin
473 of type 1 pili is assembled into a fibrillar tip structure in the *Enterobacteriaceae*.
474 Proceedings of the National Academy of Sciences. 1995;92(6):2081–2085.
475 17. Krogfelt KA, Bergmans H, Klemm P. Direct evidence that the FimH protein is the mannose-
476 specific adhesin of *Escherichia coli* type 1 fimbriae. Infection and immunity.
477 1990;58(6):1995–1998.
478 18. Collier WA, De Miranda JC. [Bacterial hemagglutination. III. Mannose inhibition of *E. coli*
479 hemagglutination]. Antonie Van Leeuwenhoek. 1955;21(2):133–40.
480 19. Hultgren SJ, Porter TN, Schaeffer AJ, Duncan JL. Role of type 1 pili and effects of phase
481 variation on lower urinary tract infections produced by *Escherichia coli*. Infection and
482 immunity. 1985;50(2):370–377.
483 20. Wright KJ, Seed PC, Hultgren SJ. Development of intracellular bacterial communities of
484 uropathogenic *Escherichia coli* depends on type 1 pili. Cellular microbiology.

485 2007;9(9):2230–2241.
486 21. Spaulding CN, Klein RD, Ruer S, Kau AL, Schreiber HL, Cusumano ZT, et al. Selective
487 depletion of uropathogenic *E. coli* from the gut by a FimH antagonist. Nature. 2017
488 22;546(7659):528–32.
489 22. Korea C-G, Badouraly R, Prevost M-C, Ghigo J-M, Beloin C. *Escherichia coli* K-12
490 possesses multiple cryptic but functional chaperone–usher fimbriae with distinct surface
491 specificities. Environmental Microbiology. 2010;12(7):1957–77.
492 23. Sohanpal BK, El-Labany S, Lahooti M, Plumbridge JA, Blomfield IC. Integrated regulatory
493 responses of fimB to N-acetylneuraminic (sialic) acid and GlcNAc in *Escherichia coli K-12*.
494 PNAS. 2004 Nov 16;101(46):16322–7.
495 24. Gally DL, Rucker TJ, Blomfield IC. The leucine-responsive regulatory protein binds to the
496 fim switch to control phase variation of type 1 fimbrial expression in *Escherichia coli* K-12.
497 Journal of Bacteriology. 1994 Sep 1;176(18):5665–72.
498 25. Kroner GM, Wolfe MB, Freddolino PL. Escherichia coli Lrp regulates one-third of the
499 genome via direct, cooperative, and indirect routes. Journal of bacteriology.
500 2019;201(3):e00411–18.
501 26. O′gara JP, Dorman CJ. Effects of local transcription and H-NS on inversion of the fim
502 switch of *Escherichia coli*. Molecular Microbiology. 2000;36(2):457–66.
503 27. Eisenstein BI, Sweet DS, Vaughn V, Friedman DI. Integration host factor is required for the
504 DNA inversion that controls phase variation in *Escherichia coli*. PNAS. 1987 Sep
505 1;84(18):6506–10.
506 28. Åberg A, Shingler V, Balsalobre C. (p) ppGpp regulates type 1 fimbriation of *Escherichia*
507 *coli* by modulating the expression of the site-specific recombinase FimB. Molecular
508 microbiology. 2006;60(6):1520–1533.
509 29. Yan M-Y, Yan H-Q, Ren G-X, Zhao J-P, Guo X-P, Sun Y-C. CRISPR-Cas12a-Assisted
510 Recombineering in Bacteria. Appl Environ Microbiol. 2017 Sep;83(17):00947-17.
511 30. Bravo V, Puhar A, Sansonetti P, Parsot C, Toro CS. Distinct mutations led to inactivation of

512 type 1 fimbriae expression in *Shigella spp*. PLoS ONE. 2015;10(3):e0121785.
513 31. Zhou K, Zhou L, Lim Q 'En, Zou R, Stephanopoulos G, Too H-P. Novel reference genes for
514 quantifying transcriptional responses of *Escherichia coli* to protein overexpression by
515 quantitative PCR. BMC Mol Biol. 2011 Apr 23;12:18.
516 32. Blomfield IC, McClain MS, Princ JA, Calie PJ, Eisenstein BI. Type 1 fimbriation and fimE
517 mutants of *Escherichia coli* K-12. Journal of Bacteriology. 1991 Sep 1;173(17):5298–307.
518 33. Van Dien S. From the first drop to the first truckload: commercialization of microbial
519 processes for renewable chemicals. Current Opinion in Biotechnology. 2013 Dec
520 1;24(6):1061–8.
521 34. Cao H, Ma Q, Chen X, Xu Y. DOOR: a prokaryotic operon database for genome analyses
522 and functional inference. Brief Bioinform. 2019 Jul 19;20(4):1568–77.
523 35. Che D, Li G, Mao F, Wu H, Xu Y. Detecting uber-operons in prokaryotic genomes. Nucleic
524 Acids Res. 2006 Apr 1;34(8):2418–27.
525 36. Richards J, Belasco JG. Obstacles to Scanning by RNase E Govern Bacterial mRNA
526 Lifetimes by Hindering Access to Distal Cleavage Sites. Molecular Cell. 2019 Apr
527 18;74(2):284-295.e5.
528 37. Laurberg M, Asahara H, Korostelev A, Zhu J, Trakhanov S, Noller HF. Structural basis for
529 translation termination on the 70S ribosome. Nature. 2008 Aug;454(7206):852–7.
530 38. Scolnick E, Tompkins R, Caskey T, Nirenberg M. Release factors differing in specificity for
531 terminator codons. Proc Natl Acad Sci U S A. 1968 Oct;61(2):768–74.
532 39. Hayes CS, Sauer RT. Cleavage of the A Site mRNA Codon during Ribosome Pausing
533 Provides a Mechanism for Translational Quality Control. Molecular Cell. 2003 Oct
534 1;12(4):903–11.
535 40. Gally DL, Bogan JA, Eisenstein BI, Blomfield IC. Environmental regulation of the fim switch
536 controlling type 1 fimbrial phase variation in *Escherichia coli* K-12: effects of temperature
537 and media. Journal of bacteriology. 1993;175(19):6186–6193.
538 41. Båga M, Göransson M, Normark S, Uhlin BE. Processed mRNA with differential stability in

539 the regulation of *E. coli* pilin gene expression. Cell. 1988 Jan 29;52(2):197–206.
540 42. Old DC, Duguid JP. Selective Outgrowth of Fimbriate Bacteria in Static Liquid Medium.
541 Journal of Bacteriology. 1970 Aug 1;103(2):447–56.
542 43. Guyer MS, Reed RR, Steitz JA, Low KB. Identification of a sex-factor-affinity site in *E. coli*
543 as γδ. In: Cold Spring Harbor symposia on quantitative biology. Cold Spring Harbor
544 Laboratory Press; 1981. p. 135–140.
545 44. Labun K, Montague TG, Gagnon JA, Thyme SB, Valen E. CHOPCHOP v2: a web tool for
546 the next generation of CRISPR genome engineering. Nucleic Acids Res. 2016 Jul
547 8;44(W1):W272–6.
548 45. König E, Zerbini F, Zanella I, Fraccascia D, Grandi G. Multiple Stepwise Gene Knockout
549 Using CRISPR/Cas9 in *Escherichia coli*. Bio-protocol. 2018;8(2):e2688.
550 46. Gonzales MF, Brooks T, Pukatzki SU, Provenzano D. Rapid Protocol for Preparation of
551 Electrocompetent *Escherichia coli* and *Vibrio cholerae*. JoVE (Journal of Visualized
552 Experiments). 2013 Oct 8;(80):e50684.
553 47. Gruber AR, Lorenz R, Bernhart SH, Neuböck R, Hofacker IL. The Vienna RNA Websuite.
554 Nucleic Acids Res. 2008 Jul 1;36(suppl_2):W70–4.
555 48. Kerpedjiev P, Hammer S, Hofacker IL. Forna (force-directed RNA): Simple and effective
556 online RNA secondary structure diagrams. Bioinformatics. 2015 Oct 15;31(20):3377–9.
557 49. Müller CM, Åberg A, Straseviçiene J, Emödy L, Uhlin BE, Balsalobre C. Type 1 fimbriae, a
558 colonization factor of uropathogenic *Escherichia coli*, are controlled by the metabolic sensor
559 CRP-cAMP. PLoS pathogens. 2009;5(2):e1000303.
560 50. Sansonetti PJ, Kopecko DJ, Formal SB. Involvement of a plasmid in the invasive ability of
561 *Shigella flexneri*. Infection and immunity. 1982;35(3):852–860.
562 51. Blomberg P, Wagner EG, Nordström K. Control of replication of plasmid R1: the duplex
563 between the antisense RNA, CopA, and its target, CopT, is processed specifically in vivo
564 and in vitro by RNase III. The EMBO journal. 1990;9(7):2331–2340.
565

566 **Table 2 Strains used in this study.**
567

Name	Strain	Reference
Wild type	*Escherichia coli* MG1655	Guyer *et al.*
S. flexneri	*Shigella flexneri 5A M90T*	Sansonetti *et al.*
Stop1	*Escherichia coli* $fimA_{106T}$	This study
Stop2	*Escherichia coli* $fimA_{T103A,T104A}$	This study
Stop3	*Escherichia coli* $fimA_{A158T,A159T,A160T,C161A,C162A}$	This study
fimA	*Escherichia coli* $fimA_{76-172}$	This study
Term1	*Escherichia coli* $fimA_{75}$*::L3S2P56*	This study
Term2	*Escherichia coli* $fimA_{1}$*::L3S2P56*	This study

569 **Table 3**. Oligos used in this study.
570

Name	Sequence	Annotation
17-0001	GGCAATCGTTGTTCTGTCGG	FimA forward
17-0002	GAAGGTCGCATCCGCATTAG	FimA reverse
17-0003	GGCTCTGTCCCTCAGTTCTACAGCGGCTCTGGCCGCTGC CtaaGACAGGTTCGTACCGCATCGCTGGCACAGGAAGGA GCAAC	FimaA deletion donor oligo forward
17-0004	GTTGCTCCTTCCTGTGCCAGCGATGCGGTACGAACCTGT CttaGGCAGCGGCCAGAGCCGCTGTAGAACTGAGGGACA GAGCC	FimA deletion donor oligo reverse
17-0005	TGCCACGACGGTTAATGGTGGGACCGTTCACTTTTAAGG GGAAGTTGTTAACGCCGCTTGCGCAGTTGAT	fimA mutant 1 stop codon crRNA1
17-0006	ATCAACTGCGCAAGCGGCGTTAACAACTTCCCCTTAAAA GTGAACGGTCCCACCATTAACCGTCGTGGCA	fimA mutant 1 stop codon crRNA1
17-0007	CTGCCACGACGGTTAATGGTGGGACCGTTCACTAAAAAG GGGAAGTTGTTAACGCCGCTTGCGCAGTTGA	fimA mutant 2 stop codon crRNA2
17-0008	TCAACTGCGCAAGCGGCGTTAACAACTTCCCCTTTTTAG TGAACGGTCCCACCATTAACCGTCGTGGCAG	fimA mutant 2 stop codon crRNA2
17-0009	GCCGCTTGCGCAGTTGATGCAGGCTCTGTTGATCTTTAA GTTCAGTTAGGACAGGTTCGTACCGCATCGC	fimA mutant 3 stop codon crRNA3
17-0010	GCGATGCGGTACGAACCTGTCCTAACTGAACTTAAAGAT CAACAGAGCCTGCATCAACTGCGCAAGCGGC	fimA mutant 3 stop codon crRNA3
17-0013	TTAGAAATAGTTTTTTGAAAGGAAAGCAGCCTCGGTACC AAATTTTCGAAAAAAGACGCTGAAAAGCGTCTTTTTTCG TTTTGGTCCGACAGGTTCGTACCGCATCGCTGGCACAGG	fimA terminator2 at ATG forward
17-0014	CCTGTGCCAGCGATGCGGTACGAACCTGTCGGACCAAAA CGAAAAAAGACGCTTTTCAGCGTCTTTTTTCGAAAATTT GGTACCGAGGCTGCTTTCCTTTCAAAAAACTATTTCTAA	fimA terminator2 at ATG reverse
17-0015	CCTGTGCCAGCGATGCGGTACGAACCTGTCGGACCAAAA CGAAAAAAGACGCTTTTCAGCGTCTTTTTTCGAAAATTT GGTACCGAGGGCAGCGGCCAGAGCCGCTGTAGAACTGAG	fimA terminator2 inside forward
17-0016	CCTGTGCCAGCGATGCGGTACGAACCTGTCGGACCAAAA CGAAAAAAGACGCTTTTCAGCGTCTTTTTTCGAAAATTT GGTACCGAGGGCAGCGGCCAGAGCCGCTGTAGAACTGAG	fimA terminator2 inside reverse
17-0017	tagatAAGGGGAAGTTGTTAACGCCGCTT	fimA crRNA2 BsaI fw
17-0018	agacAAGCGGCGTTAACAACTTCCCCTTa	fimA crRNA2 BsaI rev
17-0019	tagatATCAACAGAGCCTGCATCAACTGC	fimA crRNA3 BsaI fw
17-0020	agacGCAGTTGATGCAGGCTCTGTTGATa	fimA crRNA3 BsaI rev
17-0021	tagatAAGTGAACGGTCCCACCATTAACC	fimA crRNA1BsaI fw
17-0022	agacGGTTAATGGTGGGACCGTTCACTTa	fimA crRNA1 BsaI rev
17-0042	CTGGAACCGTAACGCAGACT	FimA 2 Fw for terminator genotyping
17-0043	AGGCAACAGCGGCTTTAGAT	FimA 2 Rv for terminator genotyping
18-0012	ATCTTTTGGGGGAAAACTGTGC	qPCR fimA Fw 90 bp recognizes all mutants
18-0013	ATTTCTAAATCGACATGGGCAGT	qPCR fimA Rv 90 bp recognizes all mutants
17-0067	TGCTGCCAATGTTTGCTCTG	fimI qPCR Fwd 233pb
17-0068	TTCACTCACCACCGTGCTAC	fimI qPCR Rev
17-0073	tacgCCAAGCTTTGAAAGGAAAGCAGCATGAAAATTAAA AC	fimA-FW cloning pSU19 HindIII EcoRI
17-0074	gccagtGAATTCTTATTGATACTGAACCTTGAAGGTCG	fimA-rv cloning pSU19 HindIII EcoRI
17-0077	tagatCGTCGCCGTCCAGCTCGACCAGGA	crRNA BsaI GFP control fw
17-0078	agacTCCTGGTCGAGCTGGACGGCGACGa	crRNA BsaI GFP control rv

571

Figure 1

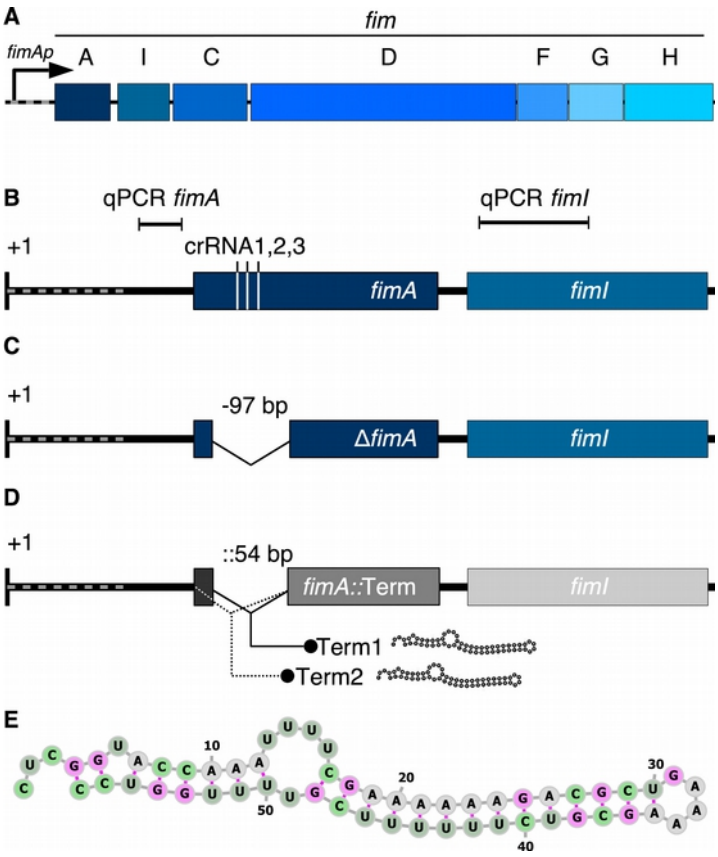

Fig 1. Design of Cas12a-dependent mutagenesis of the *fimAICDFGH* operon. A) The *E. coli fim* operon is transcribed from a promoter (fimAp) containing an invertible element (grey dotted line) and *fimA* codes for the major fimbrial subunit, which was targeted by Cas12a. B) Enhanced view of the *fim* transcript from the +1 transcriptional start site. The regions amplified for qPCR analysis in the *fimA* and *fimI* genes are shown together with the homologous positions to the three crRNAs used in this study. A stop codon was introduced to substitute the PAM sequence to generate a stop codon mutant ($fimA_{A106T}$). C) Scheme of the 97 bp *fimA* deletion (*ΔfimA*) generated with a dsDNA donor oligo bearing 40 bp of homology. D) Scheme of the 54 bp *fimA* terminator insertion generated with a dsDNA donor oligo bearing a terminator sequence surrounded by 30 bp of homology. Two different insertions were generated: the first was generated at the site of the deletion shown in C ($fimA_{75}$*::L3S2P56*) and the second at the position of the start codon ($fimA_{1}$*::L3S2P56*) of the *fimA* gene. E) Secondary structure prediction of the L3S2P56 terminator used to create the mutants shown in D.

Figure 2

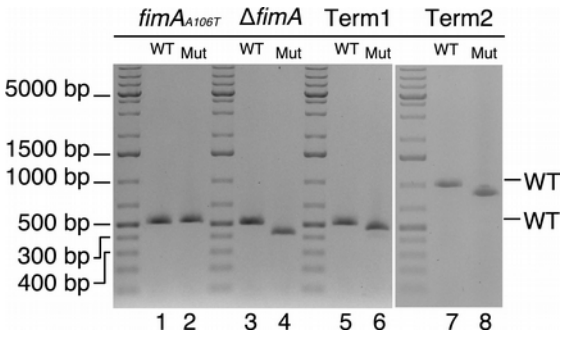

Fig. 2. Detection of *fimA* mutants by electrophoresis of PCR products. Lanes 1, 3, 5, show a 514 bp PCR product generated by primers that amplify a segment of the wild type (WT) or mutant (Mut) *fimA* gene. Lane 2 shows the unchanged migration pattern of the PCR product amplifying the stop codon mutant ($fimA_{A106T}$). Lanes 4 and 6 show the PCR product generated after amplifying DNA from the deletion mutant (*ΔfimA,* 420 bp) and the internal terminator insertion (Ter1, 474 bp), respectively. Lanes 7 show a 988 bp PCR product generated by primers that amplify a segment of wild type *fimA* including the leader sequence and lane 8 shows the 870 bp PCR product generated with DNA from the second terminator insertion (Ter2).

Supplementary Figure 1

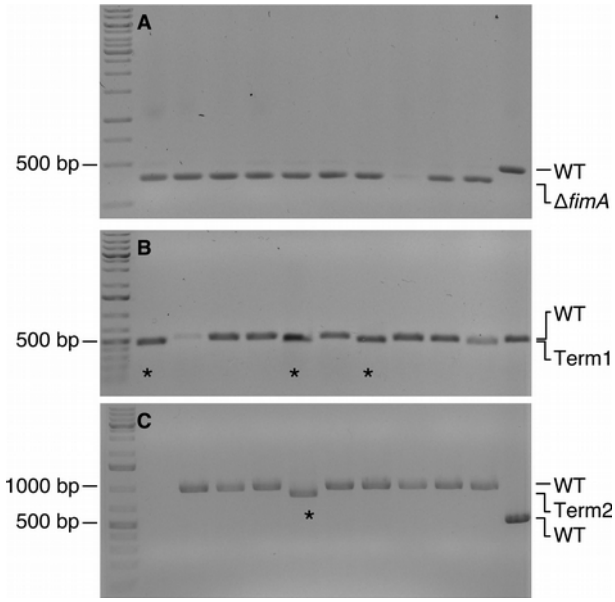

Supplementary Fig 1. Efficiency of *fimA* mutant generation with Cas12a. A) 10/10 *E. coli* colonies co-transformed with crRNA1 and the donor oligo carrying a 97 bp *fimA* deletion tested positive for a mutation as detected by colony PCR. B) 3/10 *E. coli* colonies co-transformed with crRNA1 and the donor oligo carrying a 54 bp *fimA* terminator insertion tested positive as detected by colony PCR (marked with *). C) 1/10 *E. coli* colonies co-transformed with crRNA1 and the donor oligo carrying a 54 bp terminator insertion at the *fimA* start codon tested positive as detected by colony PCR (marked with *).

Figure 3

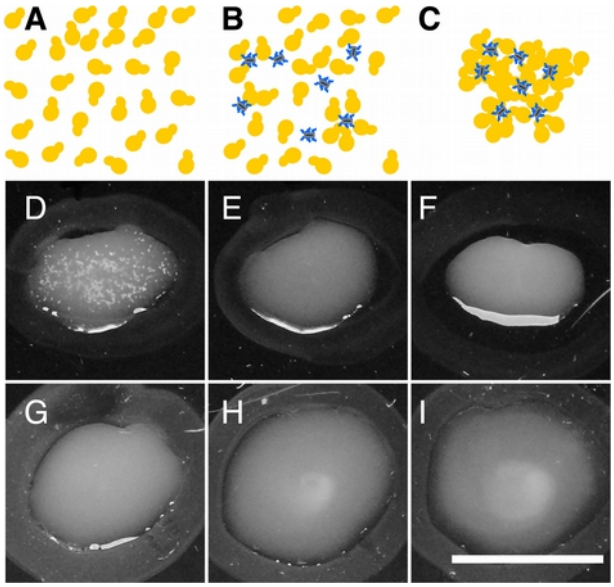

Fig 3. Agglutination assay of *fimA* mutants. A) A suspension of *Saccharomyces cerevisiae* was spread on glass plate. B) The strain to be tested was mixed. The FimH fimbriae subunit recognizes mannose residues on the surface of yeast cells. C) The polyvalent binding of fimbriae to cells causes an agglutination chain reaction, which is macroscopically visible. Agglutination reaction for the following strains: D) WT *E. coli*, E) *Shigella flexneri* M90T (negative control), F) Stop codon mutant ($fimA_{A106T}$), G) Δ*fimA,* H) $fimA_{75}$*::L3S2P56 and* I) $fimA_{1}$*::L3S2P56.* Scale bar 2 cm.

Figure 4

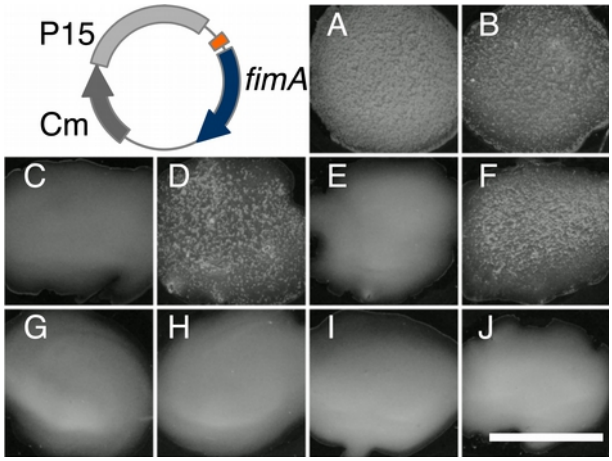

Fig 4. Plasmid complementation of *fimA* mutants. *fimA* was expressed from a plasmid under the *lac* promoter (orange). The empty vector, pSU19, was used as negative control. Agglutination reaction for the following strains: A) WT *E. coli* + empty vector, B) WT *E. coli* + *fimA* plasmid, C) $fimA_{A106T}$ + empty vector, D) $fimA_{A106T}$ + *fimA* plasmid, E) Δ*fimA* + empty vector, F) Δ*fimA* + *fimA* plasmid, *G*) Term1 ($fimA_{75}$*::L3S2P56*) + empty vector, H) Term1($fimA_{75}$*::L3S2P56*) + *fimA* plasmid, I) Term2 ($fimA_{1}$*::L3S2P56*) + empty vector, J) Term2 ($fimA_{1}$*::L3S2P56*) + *fimA* plasmid. Scale bar 2 cm.

Figure 5

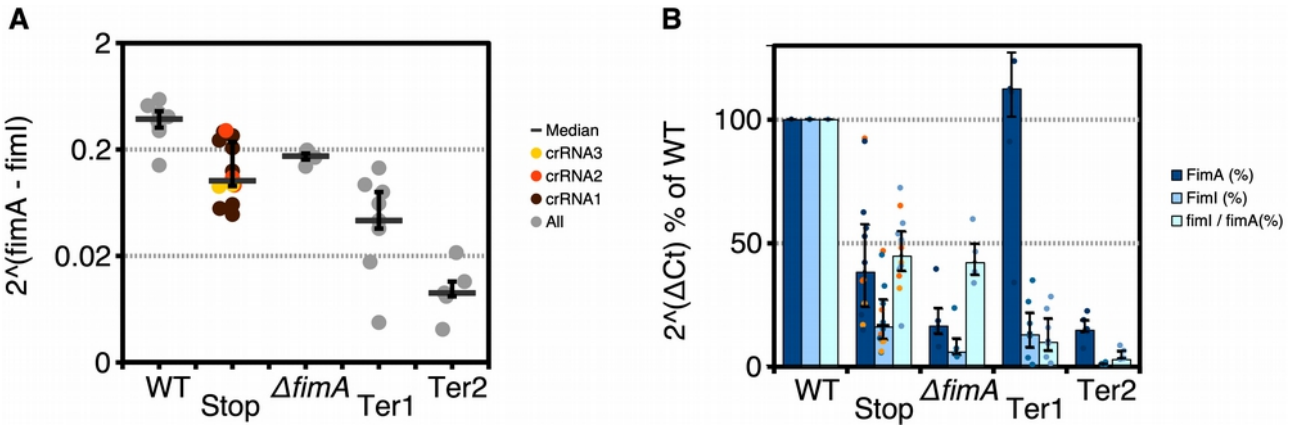

Fig 5. Quantitative PCR analysis of *fimA* and *fimI* expression. Two PCR product were used to quantify the expression of *fimA* and *fimI* (see scheme in Fig. 1). A) *fimI* expression normalized to *fimA* expression. Each data point represents a biological replicate and the median is shown (–). The error bars show the 25th and 75th percentile. B) Same data as in A) but represented as median ΔCt expression of *fimA* and *fimI* normalized to the housekeeping genes *hcaT* and *cysG* and expressed as percent of the wild type. Orange and yellow data points represent the stop codon mutants generated with crRNA1 and crRNA2 as in A. The median ratio of the normalized *fimI/fimA* expression is shown. The error bars show the 25th and 75th percentile. The labels represent the following mutants: Stop ($fimA_{A106T}$), deletion mutant (Δ*fimA*), Ter1 ($fimA_{75}$*::L3S2P56*), Ter2 ($fimA_{1}$*::L3S2P56*).

Figure 6

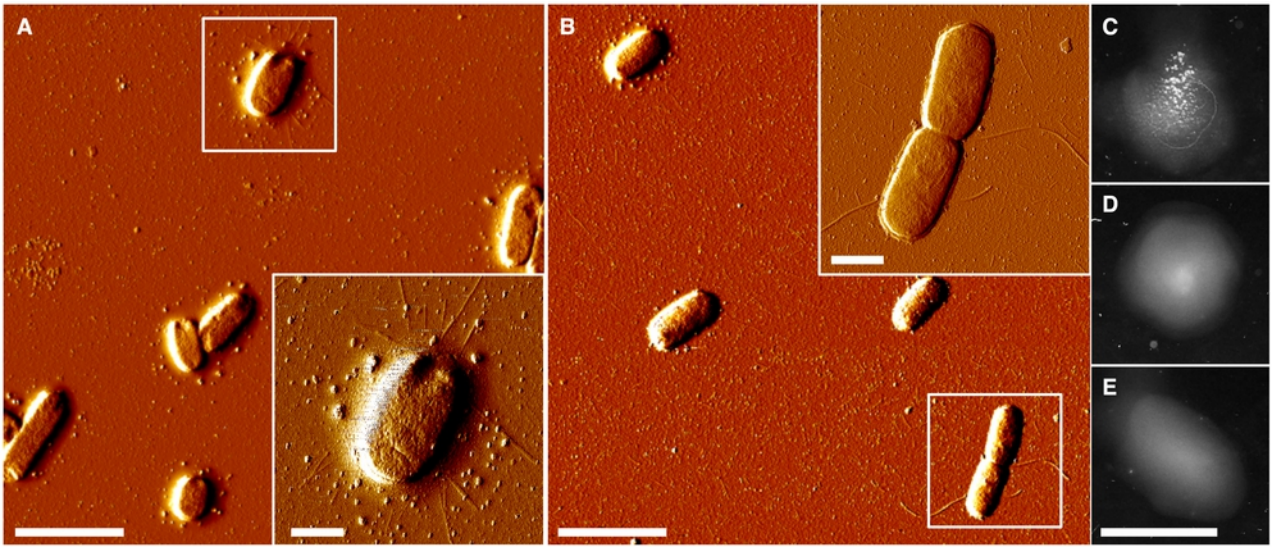

Figure 6. Atomic force microscopy (AFM) and agglutination of static cultures. A) AFM imaging of wild-type *E. coli* + *fimA* plasmid grown in static conditions. A cell showing fimbriae is shown in the inset. B) AFM imaging of Term2 mutant of *E. coli* (*fimA*$_1$*::L3S2P56*) + *fimA* plasmid grown in static conditions. A cell with flagella is shown as an inset. C) Yeast agglutination assay of wild-type *E. coli* + *fimA* plasmid grown in static conditions. D) Yeast agglutination assay of of wild-type *E. coli* + *fimA* plasmid grown in static conditions in the presence of α-methyl-mannoside. E) Yeast agglutination assay of Term2 mutant of *E. coli* (*fimA*$_1$*::L3S2P56*) + *fimA* plasmid grown in static conditions. Scale bars: A-B) 4 µm. A-B) insets 1 µm. C-E) 2 cm.